Variable density 3D Shells acquisition with an increased FOV

Y. Shu[1], and M. Bernstein[1]

[1]Department of Radiology, Mayo Clinic, Rochester, MN, United States

Introduction: Non-Cartesian 3D acquisitions often are implemented so that the center of the field of view (FOV) corresponds to the isocenter of the magnet. Sometimes, however, anatomy lies outside of the nominal FOV. To avoid spatial aliasing, techniques such as selective excitation and localized coils are used in conjunction with off-center FOV or increased FOV. In principle, off-center FOV can be implemented in any acquisition by applying phase shifts to both the transmitter and the receiver based on the gradient waveforms. Sometimes, however, off-center FOV can be challenging to implement in non-Cartesian acquisitions due to the continual variation of the readout direction, especially with a trajectory as complex as 3D shells. The shells trajectory (Fig. 1a) is a 3D non-Cartesian trajectory that samples k-space data on the surface of a group of concentric spherical shells with helical spiral interleaves. To implement off-center FOV shells, accurate synchronization between the gradient group delay and receiver delays is also required.

An alternative solution is to increase the acquired FOV. If FOV is increased while the spatial resolution is held constant, the acquisition needs to sample the k-space more densely, increasing the number of points as the *cube* of the 3D FOV, which roughly translates into a corresponding cubic increase in acquisition time. For example, if the FOV is doubled, not only are twice as many spherical shells required, but also the distance between k-space sampled points on the surface of each shell is halved, so each shell has four times as many points. The net result is $2 \times 4 = 8 = 2^3$ as many sampled points to double the FOV in three directions.

The proposed method samples only the central shells more densely, corresponding to the larger FOV, while undersampling the outer shells. This is related to an undersampled shells method that has been previously reported [1, 2], which is a 3D generalization of variable density stack of spirals [3]. The work showed that undersampling the larger radius shells that account for high frequency part of k-space can substantially reduce the acquisition time, while introducing only a modest amount of undersampling artifact, especially for high-contrast applications like CE-MRA. Here we test whether this type of variable sampling density shells acquisition can increase the FOV without paying the full price in terms of number of sampled points or acquisition time.

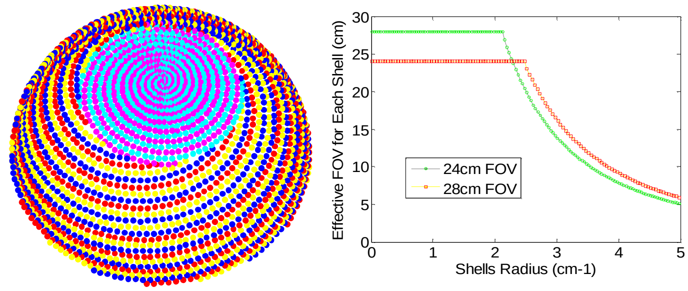

Fig. 1 a (left): A color illustration of the shells trajectory. Only one hemisphere is shown here. Multiple helical spirals are encoded with various colors. b (right): undersampling is used for both 24 and 28 cm acquisitions.

Theory and Methods: The number of interleaves is determined by the gradient hardware specifications and Nyquist sampling theorem when k-space is fully sampled. Because each shell is sampled independently from the others, there is complete freedom to adjust the sampling density for different radii of k-space.

A spoiled gradient echo shells acquisition pulse sequence was implemented for isocenter scanning. For contrast-enhanced angiography imaging, usually a 24cm FOV covers the head and superior portion of the neck. A selective RF pulse limits aliasing in the superior-to-inferior direction. However, when the object is shifted from the isocenter, e.g., by a receiver coil with a 20-50mm anterior offset, aliasing from the nose or other structures can degrade the image quality. To address the problem, a larger FOV (28 cm) is used. To satisfy the Nyquist criterion, an increase in the FOV from 24 to 28 cm would requires a 59% increase in the number of sampled points and a corresponding increase scan time, which might not be acceptable for time-constrained applications like contrast-enhanced MRA. To avoid this acquisition time penalty, we used the sampling schedule in illustrated in Fig 1b, which has a gradual decreased sampling rate for shells with radii greater than half of K_{max} (Fig. 1b). As a result, the imaging time only increased from 64 seconds to 80 seconds, or 25% instead of 59%.

A resolution phantom was scanned on a 1.5T GE scanner running 14.0 M4 software with an 8-channel head coil. The phantom was scanned with the 24 cm and 28 cm FOVs. The other imaging parameters are consistent with a CE-MRA shells protocol: TR = 7.5ms, 512 readout points, imaging matrix = 240^3 or 280^3, 1 mm isotropic image resolution, readout bandwidth = ± 64 kHz, total acquired shells number = 120 or 140.

A direct CE-MRA comparison was not feasible because it would have required two gadolinium injections on the same patient, so the flip angle is lowered from 45° to 8° to yield more signal from brain parenchyma. Instead, a healthy volunteer was scanned under an IRB-approved protocol to provide an anatomical comparison with the same two FOVs. Part of the volunteer's forehead and nose were outside of the 24cm FOV due to the anterior offset introduced by the coil.

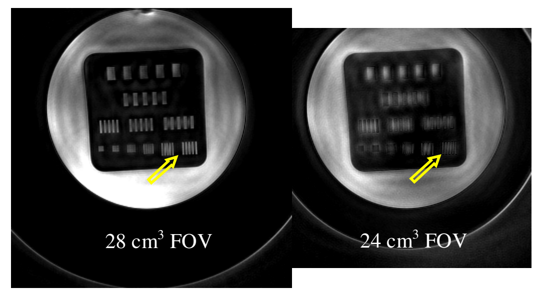

Fig. 2: Phantom experiment results shown in the same window/level. The artifacts introduced from the part of the phantom part that is outside of the FOV manifest themselves as blurring which severely decreases the image resolution (arrows).

Results: The phantom test results are shown in Fig. 2. The images obtained with the smaller FOV are corrupted due to aliasing from the part of the phantom that was shifted outside of the FOV. The resolution bars at the bottom of the phantom (arrows) better discerned with the increased FOV.

Figure 3 shows the axially reformatted images reconstructed from the volunteer acquisitions. The aliased signal intensity in the background and CSF is much lower for the 28 cm FOV acquisition because of reduced the interference from signal from outside the FOV. The average signal intensity was measured in three selected ROIs in both images for comparison. The three ROIs represent white matter, CSF and the background noise respectively. The values for all measurements are listed in Table 1.

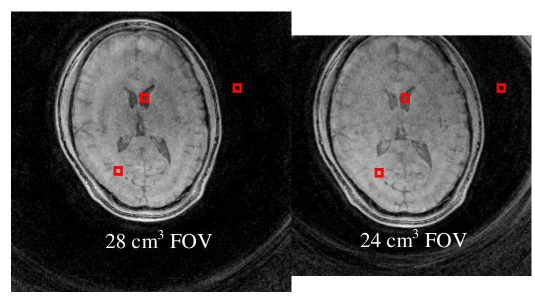

Fig. 3: Axial head image comparison from the 3D set displayed at the same window/level. Aliasing from structures like the subject's nose is more pronounced in the smaller FOV case, which reduces contrast. (Undersampling artifacts, shown as concentric rings are much less apparent on actual CE-MRA images [1] due to their higher contrast.) The average signal intensities in three regions, white matter, CSF and the background were measure in 7×7 ROIs (indicated on the figures). Their values are shown in Table 1.

Table 1: Mean ROI values comparison for the axial volunteer images

	White matter	CSF	Background
24 cm FOV	1782	997	322
28 cm FOV	1732	797	249

Conclusion: Variable density sampling for a 3D shells acquisition can be used to increase the imaging FOV with a reduced acquisition time compared to a fully-sampled acquisition strategy.

References: 1. Shu Y, Huston J, Bernstein MA, The 3D non-Cartesian Spherical Shells Trajectory, *ISMRM workshop on Non-Cartesian MRI* 2007.

2. Shu Y, Riederer SJ, Bernstein MA, *Magn Reson Med,* 2006; 56:553-562.

3. Santos JM, Cunningham CH, Lustig M, Hargreaves BA, Hu BS, Nishimura DG, Pauly JM, *Magn Reson Med* 2006;55:371-379.